Particle Accelerators, 1990, Vol. 34, pp. 25–42
Reprints available directly from the publisher
Photocopying permitted by license only

Printed in the United States of America

OVERFOCUSING IN A MIGMA AND IN EXYDER CONFIGURATIONS

H. L. BERK and H. V. WONG

Institute for Fusion Studies, The University of Texas at Austin, Austin, Texas 78712

(Received October 22, 1988; in final form April 12, 1989)

The theory of overfocusing is developed for a self-colliding storage ring (Exyder) and for a classical migma configuration. Forces due to external and self-generated equilibrium magnetic fields are considered. The band of energy containment is calculated for a model external magnetic field configuration. The forces due to self-generated magnetic fields in migmas and Exyder can also cause overfocusing, and thereby set a beta limit on a migma disc and a luminosity limit on Exyder. The luminosity in Exyder can increase substantially if the self-colliding storage ring is partially unneutralized. The beta condition of a charge-neutral thin migma limits the self-generated magnetic field to a fraction of the externally imposed magnetic field.

1. INTRODUCTION

In the migma concept[1] energetic ionized particles are stored in an axial disc so that their orbits focus close to the axis of symmetry. This can be done with particles in a vacuum magnetic field similar to that of a mirror fusion machine. These magnetic fields allow orbit containment according to the principles used for confinement of plasmas in mirror machines or confinement of particles in accelerators with weak focusing fields. For the nearly ideal case, particles are almost monoenergetic, with an angular momentum distribution in p_θ peaked about $p_\theta = 0$, and the axial velocity—the velocity component parallel to the magnetic field lines—is much less than the velocity perpendicular to the magnetic field lines. The orbits have the pattern shown in Fig. 1, where all orbits pass very close to the origin, the radial extent of the particle confinement region is two Larmor radii, and the spread in axial speed is so small that the axial extent of the migma (Δz) is much less than the Larmor radius (r_L).

The energetic ions stored in a migma establish diamagnetic currents that tend to cancel applied vacuum magnetic fields. In order to reduce the synchrotron radiation of charge-neutralizing electrons, a diamagnetic migma[2] has been proposed, in which the ion self-currents cancel the vacuum magnetic field in the bulk of the ion containment region.

Recently Blewett has suggested how a vacuum magnetic configuration could be designed so that the magnetic fields are near zero throughout most of the ion storage region. His suggestion is the basis of Exyder, a proposal for a compact self-colliding storage ring.[4]

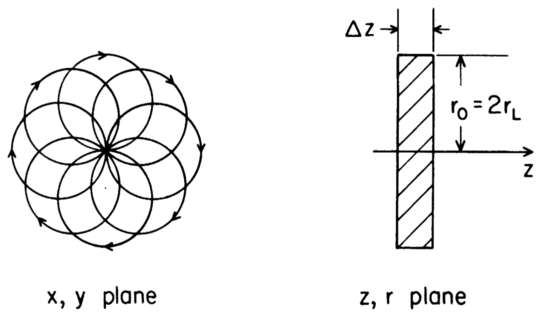

FIGURE 1 Schematic diagram of a thin migma. The ion orbits are nearly circular in shape, and for flow in the direction of the arrows the circular shape precesses clockwise. Peak currents develop at the plasma edge at $r \doteq 2r_L$ in the clockwise direction, where r_L is the ion Larmor radius. The thickness Δz of this migma is assumed to be small compared to r_L.

In the proposed diamagnetic migma of Exyder, the absence of magnetic field in the bulk of the containment region means that magnetic focusing forces are most significant when an ion reaches the radial periphery of the containment region. At the radial periphery an ion feels a magnetic force that focuses its orbit radially and axially. The radial containment condition is straightforward; there needs to be enough magnetic flux to radially reflect the particle. The purpose of this paper is to discuss why axial focusing is a more subtle problem. Of course, there needs to be a net inward axial force. However, somewhat paradoxically, one can have a condition where the inward axial force is too strong, which leads to axial expansion. We call such an effect "overfocusing."

In the Exyder configuration, ions move radially from the center, with negligible bending if the vacuum field is small, and turn around in the periphery where the magnetic field is high. Electric forces can be neglected in the presence of neutralizing, low-energy electrons that can be contained by an electric potential energy much lower than the ion energy. A schematic of the orbits is shown in Fig. 2. Inside the circle of radius r_0, the magnetic field is considered negligible and ions move in straight lines. The magnetic field abruptly rises to a mean value B_0 outside the circle (more discussion of this magnetic field is given in Section 2). Outside r_0 the particles turn in a semicircular orbit, where the radius is approximately the Larmor radius (r_L), which is small compared to r_0. In the Exyder proposal it is also assumed that the axial width Δz is small compared to r_0.

The focusing forces occur outside the radius r_0. The magnetic field is assumed to be strong enough to radially reflect the particle. The axial force felt by the particle is $F_z = \dfrac{q_0 B_r v_\theta}{c}$ (where q_0 is the ion charge, B_r the radial component of the magnetic field, v_θ the θ-component of the velocity and c the velocity of light). This force is felt during the relatively short time interval (compared to the time to more a distance $2r_0$) in which the particle is outside the radius r_0. Thus, in the time interval to turn around radially, the particle receives an inward impulse per

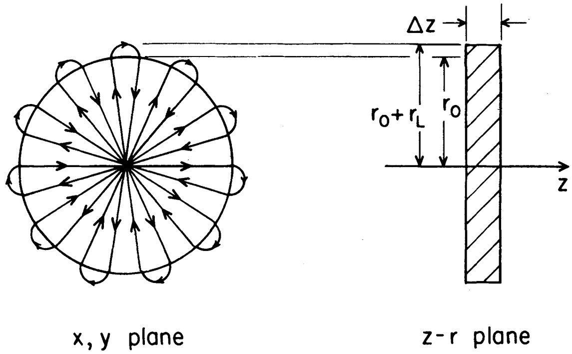

FIGURE 2 Schematic orbits in the Exyder configuration. In the low-magnetic-field $r<r_0$ region, ions move radially with little bending. At $r<r_0$, the large magnetic field bends the ions in an approximate semicircular orbit of radius r_L (the Larmor radius). Currents develop for $r>r_0$, and peak at $r \doteqdot r_0+r_L$. In this work the thickness Δz is assumed small compared to r_L.

unit mass, given by

$$\Delta v = -\oint \frac{dtq_iB_rv_\theta}{\gamma mc},$$

where m is the ion mass and $\gamma = \dfrac{1}{(1-v^2/c^2)^{1/2}}$.

We shall show that if this inward impulse is too large, then the next time the particle returns to the focusing region at the opposite side of the z-midplane, it will have a larger amplitude. Orbit instability arises when this amplitude continues to increase with multiple passes. If we assume that the axial impulse received in the focusing region is proportional to z (i.e., $I_z = -z\,\Delta v/\Delta z$ with I_z the axial impulse per unit relativistic mass and Δv the axial velocity increment received at $z=\Delta z$), then we derive from an impulse model that overfocusing arises, if

$$\frac{\Delta vT}{\Delta z}>4,$$

where T is the radial period of oscillation.

In Section 2 we describe how overfocusing can arise in a vacuum magnetic configuration that is relevant to the concept of self-colliding storage rings. For a model magnetic field we determine the energy band of good containment. We then show in Section 3 how diamagnetic effects in a standard migma configuration can also cause overfocusing. For a highly focused migma disc, the overfocusing criterion places a restriction on the beta (the ratio of average kinetic energy density to magnetic field energy density in the region occupied by energetic particles) that can be achieved. The beta limit, β_c, is found to be given roughly by

$$\beta_c \equiv \frac{2}{\ln(1/\varepsilon)},$$

where $\varepsilon = b/r_L$, with r_L the ion particle Larmor radius; $b=b_0+\Delta z$, with b_0 the mean "impact parameter" which is the mean value of the distance of closest approach to the axis of symmetry; and Δz is the axial extent of the disc. The calculation also shows that the self-magnetism of a thin axial disc-like migma configuration can produce a field only a fraction as large as the vacuum magnetic field. This means that a diamagnetic migma, where the magnetic field in the bulk of the containment region is much less than the magnetic field at the periphery, cannot be achieved for a *thin* charge-neutralized configuration. In principle, in order to achieve a diamagnetic migma as described in Ref. 2, the axial width Δz has to be large compared to the ion containment radius.

For the self-colliding storage ring, it should also be noted that as the particle number increases, the self-consistent axial self-force can also violate the overfocusing condition and thereby set a limit to the total particle storage number (hence the luminosity of the beam and the interaction rate). This limit is calculated in Section 4, and it is shown that the limiting luminosity of a large charge-neutralized storage ring does not increase with radial size. The limiting luminosity L_c scales as $L_c \propto B_0\gamma/m^2 \approx 3\,\Delta z/r_L \times 10^{40}\,\text{cm}^{-2}/\text{sec}$ if $B_0 \simeq 5T$ and $\gamma \approx 10$. (B_0 is the magnitude of the external magnetic field, γmc^2 the energy of the ions with mass m, Δz the axial extent of the disc and r_L the Larmor radius in the magnetic field.) However, a larger luminosity can in principle be obtained if one introduces compensating defocusing forces. One obvious way is to control the charge imbalance of the energetic ions and background electrons. To take this possibility into account we have included in Section 4 a model for self-generated electric fields arising from a lack of charge neutrality.

2. OVERFOCUSING IN A VACUUM MAGNETIC FIELD

Let us consider an azimuthally symmetric magnetic field which is small and nearly constant at small radii, and changes rapidly in some interval around $r \simeq r_0$ within a distance Δr as shown in Fig. 3. Such a field can be constructed by splitting two concentric solenoids as shown in Fig. 4. The field is $\mathbf{B}_0$ in the solenoidal shell, $\lambda\mathbf{B}_0$, near the axis, and significant field variation exists near $r = r_0$ when $z \lesssim \max(z_1, z_2)$.

In practice there are many variations of magnetic field coil designs to produce the fields of Fig. 3 at the z midplane. The ultimate choice should be made to economize on magnetic field energy and to optimize orbit stability.[5] However, for model studies we use magnetic fields that arise from the configuration shown in Fig. 4.

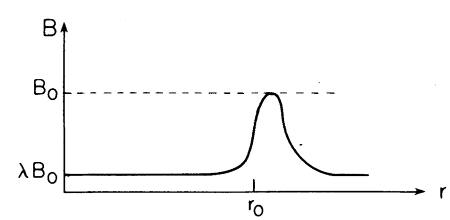

FIGURE 3 Schematic radial magnetic configuration at midplane for a self-colliding storage ring.

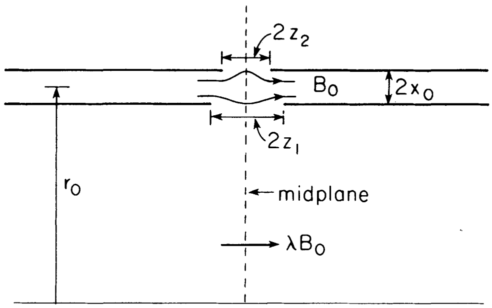

FIGURE 4 Model physical system that can establish magnetic configuration for a self-colliding storage ring. Magnetic field in sleeve is $\mathbf{B}_0$. Magnetic field in innermost solenoid is $\lambda \mathbf{B}_0$.

We only consider magnetic forces where kinetic energy does not change. Hence relativistic orbits can be evaluated from nonrelativistic theory if the relativistic mass is used instead of the rest mass. To consider orbits, we write the Hamiltonian per unit relativistic mass as

$$2H = \frac{1}{r^2}(p_\theta - q\psi/(\gamma mc))^2 + v_z^2 + v_r^2,$$

where H and p_θ are the energy and angular momentum per unit relativistic mass, and v_r and v_z the axial and radial velocities. $\psi(r, z)$ is the magnetic flux, and the magnetic field is given by

$$B_z = \frac{1}{r}\frac{\partial \psi}{\partial r}, \qquad \beta_r = -\frac{1}{r}\frac{\partial \psi}{\partial z}.$$

To solve the orbits, we assume $p_\theta \approx 0$ and that the axial speeds v_z are less than the perpendicular speeds $v_\perp \approx (2H)^{1/2}$. Then we assume that in a single radial pass through the interaction region around $r \approx r_0$, we can neglect the z motion and consider v_z constant. In this approximation, the time increment dt is

$$\begin{aligned} dt &= \frac{dr}{[2H - v_z^2 - (1/r^2)(p_\theta - q\psi(r, z)/(\gamma mc))^2]^{1/2}} \\ &\doteq \frac{dr}{[2H - (1/r^2)(p_\theta - q\psi(r, z)/(\gamma mc))^2]^{1/2}} \end{aligned} \tag{1}$$

where z and v_z are fixed. The axial acceleration is

$$a_z = \frac{qv_\theta}{\gamma mc}B_r = -\frac{q}{\gamma mcr}\left(p_\theta - \frac{q\psi(r, z)}{\gamma mc}\right)B_r,$$

and the impulse per unit mass Δv_z during a transit through the interaction region is

$$\begin{aligned} \Delta v_z &= -\int_{-T/2}^{T/2} dt \frac{q}{\gamma mc} v_\theta B_r \\ &= -\frac{2q}{\gamma mc}\int_{r_{\min}}^{r_t} \frac{dr(p_\theta - q\psi(r, z)/(\gamma mc))B_r}{[2H - (1/r^2)(p_\theta - q\psi(r, z)/(\gamma mc))^2]^{1/2}}. \end{aligned} \tag{2}$$

Here T is a radial bounce period and r_t and $r_{\min}$ are the outer radial turning point and inner turning point, respectively. Our expression is still valid if z varies appreciably in a radial bounce period, as long as z is nearly constant in the interaction region. Also note that the factor 2 in the r integral arises from accounting for positive and negative radial velocities.

To simplify Eq. (2) further, we set p_θ equal to zero, which is approximately valid if

$$p_\theta \ll q\psi(r, 0)/\gamma mc.$$

Further, given B_z, we can approximate B_r (using $\nabla \times \mathbf{B} = 0$):

$$\frac{\partial B_r}{\partial z} = \frac{\partial B_z}{\partial r},$$

which, upon integrating around the midplane, gives

$$B_r = z\frac{\partial B_z(r, z=0)}{\partial r}.$$

Then using $\psi = \int_0^r r\,dr B_z(r, z=0)$ and approximating ψ about $r = r_0$,

$$\Delta v_z = \frac{2q^2 z}{(\gamma mc)^2}\int_0^{r_t} \frac{dr(\partial B_z(r)/\partial r)\int_0^r dr' r' B_z(r')}{\left[2Hr^2 - \left(1/(\gamma mc)\int_0^r dr' B_z(r')r'\right)^2\right]^{1/2}}$$

$$\doteq \frac{2q^2 z r_0}{(\gamma mc)^2}\int_0^{r_t} \frac{dr(\partial B_z/\partial r)\left[\int_0^r dr'(B_z(r') - B_z(0)) + r_0 B_z(0)/2\right]}{\left\{2Hr_0^2 - (qr_0/(\gamma mc))^2\left[\int_0^r dr'(B_z(r') - B_z(0)) + B_z(0)r_0/2\right]^2\right\}^{1/2}} \quad (3)$$

Note that if the fields increase at small r, the numerator is positve; the contribution to Δv_z is positve and therefore axially defocusing. At large radii, $\partial B_z/\partial r$ is negative, which contributes to axial focusing if the particle can reach this region. The stagnation that arises in the region where a particle turns radially tends to be strongly weighted because the denomintor of Eq. (3) vanishes there. If this region is where $\partial B_z/\partial r > 0$, one tends to obtain a strong axial focusing contribution that overcomes the defocusing contribution from the smaller radii.

To cast the expression in a more dimensionless form, we define $b(r) = B_z(r)/B_0$, $\omega_{c0} = qB_0/\gamma mc$, with B_0 the characteristic magnetic field at $r \approx r_0$, and $r_L = (2H)^{1/2}/\omega_{c0} \equiv$ the Larmor radius for a particle of energy H in uniform magnetic field B_0.

Then we find

$$\frac{\Delta v_z}{\omega_{c0} r_0} = \frac{2z}{r_0}\int_0^{r_t} \frac{dr\frac{\partial b(r)}{\partial r}\left\{\int_0^r dr'[b_0(r') - b(0)] + (r_0/2)b(0)\right\}}{\left\{r_L^2 - \left[\int_0^r dr'(b(r) - b(0)) + (r_0 b(0)/2)\right]^2\right\}^{1/2}}$$

$$\equiv -\frac{Iz}{r_0}. \quad (4)$$

This expression depends strongly on energy. The low-energy particles are turned before they reach the region $\partial B_z/\partial r < 0$, and since I is intrinsically negative for such particles they cannot be contained axially. Higher energy particles have positive I, hence are focusing axially. We also restrict r_L so that

$$r_L < \max\left(\frac{1}{r}\int_0^r drrb(r)\right) \approx \frac{1}{r_0}\int_0^\infty drrb(r),$$

which guarantees radial focusing. This follows from the Hamiltonian when $p_\theta = 0$, as then

$$v_r^2 \leq 2H - \left(\frac{q\psi}{\gamma mcr}\right)^2 \equiv \omega_{c0}^2\left[r_L^2 - \frac{1}{r^2}\left(\left(\int_0^r drrb(r)\right)^2\right]\right.$$

As we assume $r_L < \max\left(\int_0^r drb(r)r\right)$, there is a point r_0 where $r_L^2 = \frac{1}{r_0^2}\int_0^{r_0} r\,drb(r)$. For small r, $\frac{1}{r^2}\left(\int_0^{r_0} r\,drb(r) \div b^2\frac{(0)r^2}{4}\right)$. Therefore $v_r^2 > 0$ for small r, and v_r^2 must vanish at a point $r = r_t < r_0$. Thus, the radial containment region (the region where $v_r^2 > 0$) is limited to a radius less than r_0.

We now develop a mapping technique to study axial focusing if $I > 0$. Suppose a particle is at $z = z_n$ with an axial speed $v_z = v_n$ when it is about to enter the interaction region $r \simeq r_0$. Upon passing through the interaction region it receives an impulse

$$\Delta v_z = -\omega_{c0} I z_n,$$

so its coordinates will be $z = z_n$ and $v_{n+1} = v_n - \omega_c I z_n$. If a radial bounce period T nearly elapses ($T \approx (4/\lambda\omega_c 0)\sin^{-1}(\lambda r_0/2r_L)$ and λB_0 is the magnetic field at small radii), the particle will again be ready to enter the interaction region, and its coordinates will be,

$$\begin{aligned} z_{n+1} &= z_n + v_{n+1}T \\ v_{n+1} &= v_n - \omega_{c0} z_n I \end{aligned} \tag{5}$$

The stability of this difference equation is found by seeking normal mode solutions $z_{n+1} = \Lambda z_n$, $v_{n+1} = \Lambda v_n$. Then solving Eq. (5) leads to the dispersion relation

$$\Lambda^2 - (2 - 4f)\Lambda + 1 = 0,$$

where $f = \Delta v_z T/4z_n = \omega_{c0} TI/4$. The solutions for Λ are

$$\Lambda = 1 - 2f \pm i2(f - f^2)^{1/2}.$$

Stability requires $|\Lambda| > 1$, which restricts f to the interval $0 < f < 1$. Satisfying the left side of the inequality is the condition for focusing. Satisfying the right-hand side is the condition for avoiding "overfocusing."

In overfocusing, the impulse is so large that a particle achieves a larger amplitude in $|z_n|$ with each axial impulse, with the sign of z_n alternating with each kick. It can be readily shown that for the critical case $f = 1$, a particle with a velocity $v_n = 2z_n/T$ and axial position $z = z_n$ receives an impulse $-4z_n/T$ and at its next interaction its coordinates are $v_{n+1} = -2z_n/T = -v_n$ and $z_{n+1} = -z_n$. It also follows that at $f = 1$ the particle passes through the origin when it passes through the axis. Any larger impulse will cause an exponential increase of the coordinates

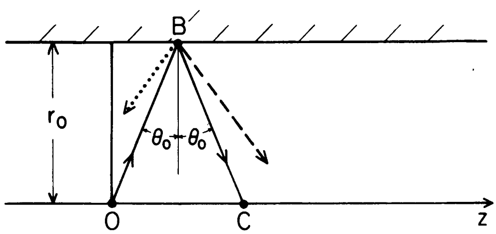

FIGURE 5 Focusing, defocusing and overfocusing trajectories. If point 0 is the origin of a "lens" with reflection symmetry, then a trajectory emerging from 0 is a focusing one, if on reflection at B it lies within the angle $0BC$. The trajectory is defocusing if on reflection at B it lies to the right of BC (the dashed line). The trajectory is overfocusing if on reflection at B it lies to the left of $0B$ (dotted line).

with successive interactions. These observations are consistent with a physical interpretation given by Blewett (private communication) for overfocusing. He considers a particle moving from the origin at a point 0 in Fig. 5. The particle moves in a straight line until it reaches the point B at radius r_0. For $r > r_0$, the particle feels a strong focusing force causing the particle to reflect radially, and having its v_z component changed. The particle returns to $r < r_0$ near the point B. The line BC is the line of specular reflection. If the reflected trajectory returns on the dashed line, to the right of the line BC, we have a defocused system, while if the trajectory returns on the dotted line, to the left of OB, we have an overfocused system.

It can also be shown that if a continuously applied focusing force is added to the impulsive focusing force considered here, the value of f for which overfocusing occurs decreases. Hence, the external mirror fields makes the overfocusing condition slightly more restrictive. To counter overfocusing, one must compensate with defocusing forces.

It is also interesting to study Eq. (4) when f is small and the difference scheme can therefore be converted to a differential equation. We have

$$\frac{dz}{dt} \doteq \frac{z_{n+1} - z_n}{T} \doteq v_z$$

$$\frac{dv_z}{dt} \doteq \frac{v_{n+1} - v_n}{T} \doteq \frac{4fz}{T^2}. \tag{6}$$

Combining these equations yields

$$\frac{d^2z}{dt} + \frac{4f}{T^2} z = 0. \tag{7}$$

Hence, the solution is

$$\begin{aligned} z &= z_0 \cos(\omega_z t + \phi) \\ v_z &= -\omega_z z_0 \sin(\omega_z t + \phi), \end{aligned} \tag{8}$$

with

$$\omega_z = \frac{2f^{1/2}}{T}.$$

In practice, one may have a condition that particles must be stored within a distance Δz. The axial spread in velocity then must satisfy

$$\frac{v_{z0}^{0}}{v_{\perp 0}^{2}} < \frac{\Delta z^2 \omega_z^2}{v_{\perp 0}^2} = \frac{\Delta z^2}{r_L^2}\frac{I}{\omega_{c0}T}$$
$$\approx \begin{cases} \dfrac{\Delta z^2}{2\pi r_L^2} I, & \text{if } \dfrac{\lambda R_0}{2r_L} \approx 1 \\ \dfrac{\Delta z^2 I}{2r_L r_0}, & \text{if } \dfrac{\lambda R_0}{2r_L} \ll 1 \end{cases} . \qquad (9)$$

To illustrate the relevance of the orbit stability criteria, we consider the model field discussed at the beginning of the this section and illustrated in Fig. 4. Away from slots, the magnetic field in the sleeve is $\mathbf{B}_0$ and the magnetic field in the central region is $\lambda \mathbf{B}_0$. Thus, the current density at $r = r_0 + \Delta x$ is $cB_0/4\pi$, while at $r = r_0 - \Delta x$ the current density is $cB_0(1-\lambda)/4\pi$. We calculate the magnetic flux $\psi(r, z) = \int_0^r dr\, rB_z(r, z)$ in the vicinity of the slit assuming $2z_0 \approx 2x_0 \ll r_0$. The solution consists of the superposition of current densities

$$\mathbf{J} = \mathbf{J}_1 + \mathbf{J}_2$$

where

$$\mathbf{J}_1 = \frac{cB_0}{4\pi}\delta(r - r_0 - x_0)\hat{\theta} - \frac{(1-\lambda)cB_0}{4\pi}\delta(r - r_0 + x_0)\hat{\boldsymbol{\theta}} \qquad (10)$$

and

$$\mathbf{J}_2 = -\frac{cB_0}{4\pi}\delta(r - r_0 - x_0)\theta(|z| - z_2)\hat{\boldsymbol{\theta}} + \frac{(1-\lambda)cB_0}{4\pi}\delta(r - r_0 + x_0)\theta(|z| - z_1)\hat{\boldsymbol{\theta}}. \qquad (11)$$

The exact solution for the magnetic flux function ψ_1, as well as the approximate solution in the vicinity of $r \approx r_0$, is

(a) $r \le r_0 - x_0$

$$\psi_1(r, z) = \lambda B_0 \frac{r^2}{2} \div \lambda B_0 r_0 x + \lambda \frac{B_0 r_0^2}{2}$$

(b) $r_0 + x_0 < R < r_0 - x_0$

$$\psi_1(r, z) = \lambda B_0 \frac{(r_0 - x_0)^2}{2} + \frac{B_0}{2}[r^2 - (r_0 - x_0)^2]$$
$$\div \lambda \frac{B_0 r_0^2}{2} + B_0 r_0 (x + x_0) - \lambda B_0 r_0 x_0$$

(c) $r > r_0 + x$.

$$\psi_1(r, z) = B_0 \frac{(r_0 - x_0)^2}{2} + 2B_0 r_0 x_0$$
$$\div \lambda \frac{B_0 r_0^2}{2} + 2B_0 r_0 x_0 - \lambda B_0 r_0 x_0, \qquad (12)$$

where we define $x = r - r_0$ and, in the approximate forms, we have neglected term $O(x_0^2)$.

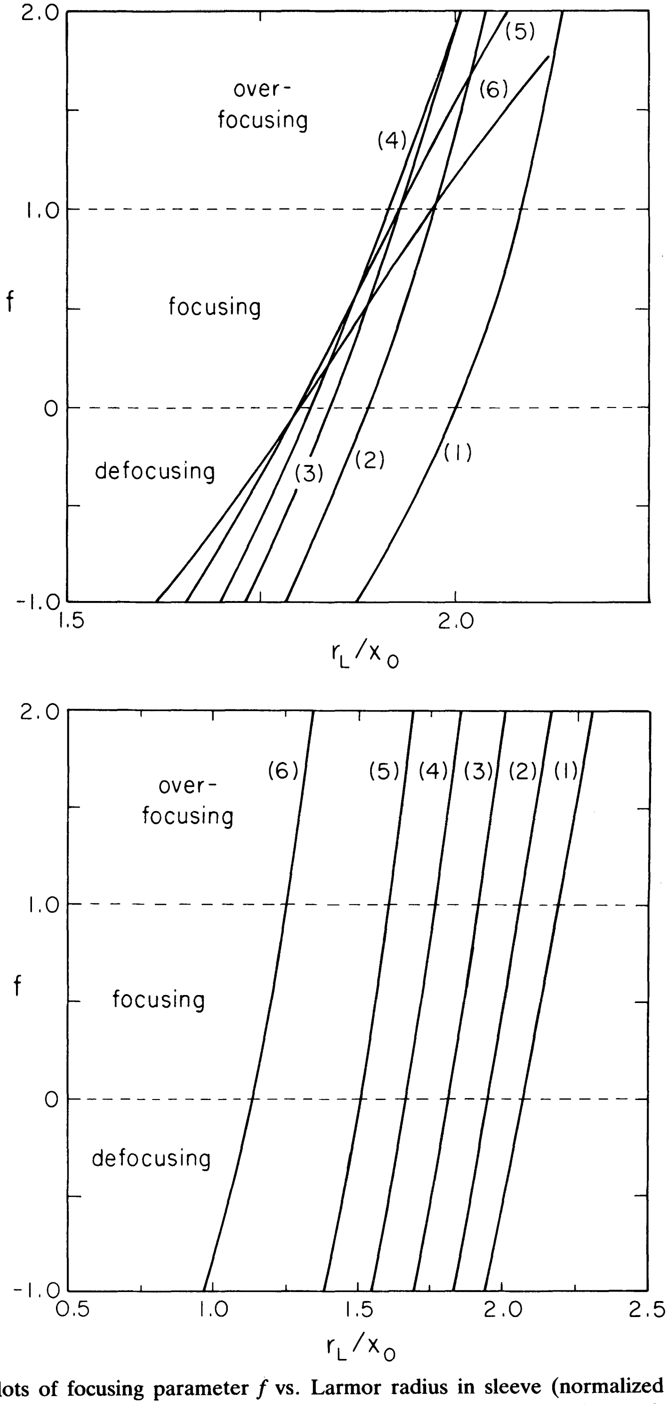

FIGURE 6 Plots of focusing parameter f vs. Larmor radius in sleeve (normalized square root of energy) with $\lambda = 0.1$ and $r_0/x_0 = 10$. In (a) $z_1 = z_2$ and each curve is for a given value of z_2/x_0. For curves (1)–(6) the values of z_2/x_0 are: 0.25, 0.5, 0.75, 1.2, 1.5, 2.0, respectively. In (b) $z_2 = x_0$ and in the curves (1)–(6) the values of z_1/z_2 are 0.5, 0.75, 1.0, 1.25, 1.5, 2.0, respectively.

For the current $\mathbf{J}_2$, we neglect cylindrical effects for evaluating ψ_2 in the vicinity of $r \approx r_0\,|z| \approx z_1, z_2$. Then, treating $\mathbf{J}_2$ as a current in a fixed direction, we have

$$\psi_2(r, z) \doteqdot \frac{-cr_0B_0}{4\pi}\int_{-\infty}^{\infty} dy\left[\int_{-z_2}^{z_2} \frac{dz'}{[(z-z')^2+y^2+(x-x_0)^2]^{1/2}} - \int_{-z_1}^{z_1} \frac{dz'(1-\lambda)}{[(z-z')^2+y^2+(x+x_0)^2]^{1/2}}\right]. \tag{13}$$

These integrals can be evaluated straightforwardly. For the integrals in Eq. (3) we then find

$$\begin{aligned}\frac{1}{B_0}\int_0^r dr'r'B_z(r,0) &\equiv \frac{1}{B_0}[\psi_1(r,0)+\psi_2(r,0)] = r_0\left\{\frac{z_2}{2\pi}\ln\left[\left(\frac{x}{x_0}-1\right)^2+\frac{z_2}{x_0^2}\right]\right. \\ &- \frac{(1-\lambda)r_0z_1}{2\pi}\ln\left[\left(\frac{x}{x_0}+1\right)^2+\frac{z_1^2}{x_0^2}\right] \\ &\left.+\frac{1}{\pi}(x-x_0)\tan^{-1}\left(\frac{z_2}{x-x_0}\right)-\frac{(1-\lambda)}{\pi}(x-x_0)\tan^{-1}\left(\frac{z_2}{x-x_0}\right)\right\}+\frac{\psi_1(r)}{B_0},\end{aligned} \tag{14}$$

with $\psi_1(r)$ given in Eq. (12); and

$$\frac{1}{B_0}\frac{\partial B_z}{\partial r} = \frac{\partial B_r}{B_0\partial z} = \frac{1}{B_0r_0}\frac{\partial^2\psi}{\partial z^2} = \frac{1}{\pi}\left[\frac{z_2}{(x-x_0)^2+z_2^2} - \frac{(1-\lambda)z_1}{(x+x_0)^2+z_1^2}\right]. \tag{15}$$

We substitute Eqs. (13) and (14) into Eq. (3) [or Eq. (4)] and evaluate the integral for I numerically. The relevant integral for orbit stability is $f = \omega_{c0}TI/4$, so stable orbits lie in the interval $0<f<1$. Note that $f<0$ is an unfocused orbit and $f>1$ is an overfocused orbit. The values of f as a function of r_L are given in Figs. 6(a) and (6b). In Fig. (6a) $z_1 = z_2$ and the various curves are for different values of z_1/x_0. In Fig. (6b) we choose $z_1 = x_0$ and the curves are for various z_2/z_1. The most dramatic aspect of those curves is their steepness as a function of r_L. Roughly, these curves indicate that focused orbits occur in an energy interval $\Delta E/E_0 \approx 10\%$ where ΔE is the spread of energy about an energy E_0 (where, say $f = 1/2$). This steepness in the energy dependence of f can be mitigated with careful magnetic field design as indicated by Blewett.[5] Nonetheless, the example shows that overfocusing is an important phenomenon in orbit stability.

3. OVERFOCUSING BY SELF-MAGNETIC FIELDS IN A MIGMA

We now show how overfocusing can arise in a self-consistent equilibrium, and we take a nearly ideal migma disc as an example. An ideal migma is a thin disc with axial length Δz much less than the radius $r_0 \doteqdot 2r_L$. All particles are nearly monoenergetic with a speed v and have p_θ values close to zero. The equilibrium density n of an ideal migma is determined from the condition $nv_r = \text{constant}$ with $v_r = [2H - (q\psi/m\gamma_c^2]^{1/2}$. In a nearly uniform magnetic field B_0, i.e.

$2r_L(1/B)(\partial B_z/\partial r) \ll 1$, n is then given by

$$n = \frac{2\bar{n} r_L \sigma(r)}{\pi r}. \tag{16}$$

Here $\sigma(t) = (1 - r^2/4r_L^2)^{-1/2}$, where r_L is the ion Larmor radius and equals v/ω_c, and $\omega_c = \dfrac{qB_0}{\gamma mc}$. The mean density averaged over a cross-sectional area is $\bar{n}$.

Notice that the density of an ideal migma is singular at the origin and at $r = 2r_L$. There are no particles at $r > 2r_L$. By considering a distribution function of finite width in p_θ and finite energy, these singularities are replaced by finite peaked functions. Examples of such finite peaked functions can be found in Ref. 6, and a nonsingular form for $\sigma(r)$ can be used when there is a small spread. For example, given a distribution of particles with a characteristic impact parameter b (i.e., b is the characteristic distance of closest approach of a particle to the origin) one finds that

$$\frac{\sigma(r)}{r} \to \frac{1}{r(1 - r^2/4r_L^2)^{1/2}} \quad \text{if} \quad b \ll r \ll 2r_L - b$$

$$\frac{\sigma(r)}{r} \approx \frac{1}{b} \quad \text{if} \quad r \lesssim b$$

$$\frac{\sigma(r)}{r} \approx \frac{1}{r_L b^{1/2}} \quad \text{if} \quad 2r_L - r \approx b$$

$$\frac{\sigma(r)}{r} \to 0 \quad \text{if} \quad r - 2r_L \gg b.$$

The directed speed is $v_\theta = -\omega_c r/2$, so the current density j_θ is

$$j_\theta = nqv_\theta = -\frac{\bar{n} q r_L \omega_c \sigma(r)}{\pi}. \tag{17}$$

Note that for an ideal migma, j_θ is singular at $r = 2r_L$. For a distribution function with a spread in p_θ and energy, j_θ is peaked but finite around $r = 2r_L$.

For simplicity we take $\bar{n}$ constant between $-\Delta z/2 < z < \Delta z/2$. Our model can be further refined to allow Δz to be a function of r, and we can even attempt to find an explicit distribution function whose density will replicate this property. However, the essential aspects of our model are that we have a thin disc of characteristic width $\Delta z \ll r_L$, and that $\partial n/\partial z$ vanishes on the mid-plane. The induced magnetic fields produced inside the containment region of a general distribution will be quite similar to what is produced in the model we analyze.

The induced magnetic field, $\mathbf{B}_1$, is given by the equations

$$\frac{\partial B_{1r}}{\partial z} - \frac{\partial B_{1z}}{\partial r} = \frac{4\pi}{c} j_\theta = -\frac{4\bar{n} r_L q \omega_c \sigma(r)}{c} \tag{18}$$

$$\nabla \cdot \mathbf{B}_1 \equiv \frac{\partial B_{1z}}{\partial z} + \frac{1}{r}\frac{\partial (rB_{1r})}{\partial r} = 0. \tag{19}$$

As the axial variation is rapid, we can neglect $(\partial B_{1z}/\partial r)$ in Eq. (18), so B_r is found to be

$$B_{1r} = -\frac{4\bar{n}r_L q\omega_c z\sigma(r)}{c} = -\frac{B_0\bar{\beta}z\sigma(r)}{2\pi r_L}, \qquad |z| < \frac{\Delta z}{2}, \tag{20}$$

where $\bar{\beta} = \gamma 8\pi\bar{n}mv^2/B_0^2$ is the mean beta averaged over cross-sectional area of the particles in the migma. We note that the evaluation of B_{1r}, given Eq. (20), fails near the edge of an ideal migma when $2r_L - r \leqslant \Delta z$. This is because, in this case, $\partial B_{1z}/\partial r$ cannot be neglected in Eq. (18), as can be ascertained by calculating $\dfrac{\partial B_{1z}}{\partial z} \approx \dfrac{B_{1z}}{\Delta z}$ in Eq. (19). However, the expression for B_{1r} at $r \approx 2r_L$ is valid if $\Delta z < \sigma/(\partial\sigma/\partial r)$, and this can be achieved if there is enough speed in, say, p_θ.

We note that $B_{1r}/B_0 \approx \beta z/r_L$, which needs to be small to justify neglecting self-fields in the equilibrium. Thus consistency requires that $\bar{\beta}\,\Delta z/r_1 \ll 1$. It can also be shown that $B_{1z}/B_0 \ll \bar{\beta}\,\Delta z \ln(\Delta z/r_L)/r_L$. Thus, with $\bar{\beta} \approx 1$, we still have small self-field effects if $\Delta z/r_L \ll 1$.

The axial acceleration felt by a particle is

$$a = \frac{F_z}{\gamma m} = -\frac{qv_\theta}{\gamma mc} \quad B_{1r} = -\frac{\bar{\beta}}{4\pi}\frac{\omega_c^2 zr\sigma(r)}{r_L}, \tag{21}$$

where we have used Eq. (20) and $v_\theta = -\omega_c r/2$. The axial impulse per unit relativistic mass this particle receives in passing through the outer radial periphery is, using Eq. (12),

$$\Delta v = \int a\,dt = -\frac{\bar{\beta}}{4\pi}\frac{\omega_c^2}{r_L}\int dtzr\sigma(r). \tag{22}$$

Let us assume z is nearly constant in passing through the outer periphery. Then,

$$dt \doteqdot \frac{dr}{v_r}\bigg|_{z=\text{const.}} = \frac{2\,dr}{\omega_c(4r_L^2 - r^2)^{1/2}}. \tag{23}$$

Thus,

$$\Delta v = \frac{-2\bar{\beta}}{\pi}z\omega_c\int_{2r_L-r'}^{2r_L-\varepsilon r_L}\frac{r\,dr}{(4r_L^2 - r^2)} \doteqdot \frac{-\bar{\beta}}{\pi}\omega_c z\ln\left(\frac{1}{\varepsilon}\right), \tag{24}$$

where dt is multiplied by a factor of two to take into account the positive and negative radial velocities. The cut-off εr_L is introduced in order to take account of the logarithmic singularity and $r_L \gg 2r_L - r' \gg \varepsilon$, the natural spread that exists in a nonideal migma. With the natural spreads, the expression for Δv is not divergent. By determining the limiting values where Eq. (24) is applicable, the magnitude of the large logarithmic response is found. Our calculation is only accurate to the extent $\ln(1/\varepsilon)$ is large. Two natural spreads determine the cutoff; $\Delta r(\Delta r \approx \sigma(r)/\partial\phi/\partial r$ at $r \approx 2r_L)$ and Δz with $\varepsilon r_L < \max(\Delta r, \Delta z)$. To logarithmic accuracy we can choose $\varepsilon r_L = \Delta r + \Delta z$ and incorporate both cases.

We have noted that, when $\Delta z > \Delta r$, our expression for B_{1r} fails when $2r_L - r \lesssim \Delta z$. A proper evaluation of B_{1r} would lead to a nondivergent contribution in Eq. (24) for $r \doteqdot 2r_L$; the appropriate integration of this term would correct the logarithmic term proportional to $\ln(1/\varepsilon)$. We do not attempt to find this correction. If $\Delta r > \Delta z$, the cut-off parameter can be calculated relatively simply. In this case we note that B_{1r} can be obtained without any local breakdown of the expression, and we have near $r = 2r_L$,

$$B_{1r} = z\frac{4\pi j_\theta}{c} \doteqdot \frac{-2\pi}{c}\omega_c rqn(r)z.$$

We now define a phase space mean of a physical quantity $G(p_\theta, H, r)$ as

$$\bar{G} = \frac{\int dp_\theta\, dHGF(p_\theta, H)}{\int dp_\theta\, dHF(p_\theta, H)}. \tag{25}$$

For highly peaked distributions, all particles have nearly the same G value, so $\bar{G}$ characterizes the typical value of G. Now let G be the impulse Δv, so the mean impulse $\overline{\Delta v}$ is

$$\overline{\Delta v} = \frac{-\int dp_\theta\, dHF(p_\theta, H)\int dtqv_\theta B_{1r}/\gamma mc}{\int dp_\theta\, dHF(p_\theta, H)}$$

$$\doteqdot \frac{-(2\pi qz\omega_c^3/cB_0)\int dp_\theta\, dHF(p_\theta, H)\int_{r_{\min}}^{r_{\max}} drr^2n(r)/v_r}{\int dp_\theta\, dHF(p_\theta, H)}$$

$$= \frac{-2\pi qz\omega_c^3}{cB_0}\frac{\int_0^\infty drr^3n^2(r)}{\int dp_\theta\, dHF(p_\theta, H)}, \tag{26}$$

where $r_{\min}$ should satisfy the condition

$$1 \ll \frac{r_{\min}}{\Delta r} \ll \frac{2r_L}{\Delta r} - 1.$$

However, the logarithmic accuracy of the last term in Eq. (26) is not affected by replacing $r_{\min}$ by zero where we have used $\int (dp_\theta\, dH/v_r)F(p_\theta, H) = rn(r)$. We note that $\int_0^\infty dr\, r^2n(r)$ is logarithmically large from the contribution near $r \approx 2r_L$. For example, the distribution function

$$F(p_\theta H) = \frac{\bar{\beta}B_0^2}{4\pi^2\gamma_m\omega_c}\delta\left(H - \frac{v_0^2}{2}\right)\theta\left(\frac{p_\theta^2}{v^2} - b_0^2\right)$$

characterizes a spread of impact parameters of width b_0; the normalization constant is chosen to produce a migma with a mean beta value $\bar{\beta}$ (if $b_0 \ll r_L = v_0/\omega_c$). Here $\theta(x)$ is a step function. Using Eq. (26), the mean impulse on a particle is then found to be

$$\overline{\Delta v} = -\frac{2\bar{\beta}\omega_c z}{\pi}\int_0^{2+\varepsilon} dx x^3 c^2(x, \varepsilon)$$

where $c(x, \varepsilon)$ is a normalized density which is a function of the radial coordinate $r = xr_L$ and the parameter $b_0 = \varepsilon r_L$. Specifically, $c(x, \varepsilon)$ is given by[6]

$$c(x, \varepsilon) = \frac{1}{2x\varepsilon}\int_{-\varepsilon}^{\varepsilon} \frac{d\varepsilon'\theta\left(4 - \frac{1}{x^2}(x^2 - 2\varepsilon')^2\right)}{\left[4 - \frac{1}{x^2}(x^2 - 2\varepsilon')^2\right]^{1/2}}$$

$$= \frac{1}{4\varepsilon}\begin{cases} \pi, & 0 < x < \varepsilon \\ \sin^{-1}\left[\frac{2+\varepsilon}{2}\left(\frac{\varepsilon}{x} - \frac{x}{2+\varepsilon}\right)\right] + \sin^{-1}\left[\frac{(2-\varepsilon)}{2}\left(\frac{\varepsilon}{x} + \frac{x}{2-\varepsilon}\right)\right]; & \varepsilon < x < 2-\varepsilon \\ \sin^{-1}\left[\frac{2+\varepsilon}{2}\left(\frac{\varepsilon}{x} - \frac{x}{2+\varepsilon}\right)\right] + \frac{\pi}{2}; & 2-\varepsilon < x < 2+\varepsilon \end{cases}$$

To compare the result of a finite density profile with the ideal case, with cut-offs introduced as given by Eq. (24), we compare the function $Q_I(\varepsilon) \equiv \frac{1}{2}\ln(1/\varepsilon)$ with the integral $Q_s(\varepsilon) \equiv \int_0^{2+\varepsilon} dx x^3 c^2(x, \varepsilon)$. We find:

$$Q_I(0.001) = 3.45$$
$$Q_I(0.01) = 2.30$$
$$Q_I(0.1) = 1.15$$

while

$$Q_s(0.001) = 4.55$$
$$Q_s(0.01) = 3.40$$
$$Q_s(0.1) = 2.25.$$

Empirically, we find the difference $Q_s(\varepsilon) - Q_I(\varepsilon) = 1.1$, independent of ε. Note that the numerical results give a slightly larger $\overline{\Delta v}$ than the analytic estimate by an amount independent of ε. Thus we see that the results obtained by taking finite radial spread into account yield results compatible with our cutoff procedure.

We now determine the overfocusing condition using our analytic estimate. The radial bounce time is $T = 2\pi/\omega_c$. Thus, using $\Delta v T > 4z$, we find that the overfocusing instability arises in a disc-like migma when

$$\frac{\Delta v}{z}\left(\frac{2\pi}{\omega_c}\right) > 4$$

or

$$\bar{\beta} > \frac{2}{\ln(1/\varepsilon)}. \tag{27}$$

The validity of this prediction requires that

$$\bar{\beta}\frac{\Delta z}{r_L}=\frac{2\varepsilon'}{\ln(1/\varepsilon)}<1, \tag{28}$$

where $\varepsilon'=\Delta z/r_L$.

The overfocusing condition then indicates that the disc must swell axially if $\bar{\beta}$ is to be increased.

4. OVERFOCUSING BY SELF-MAGNETIC FIELDS IN STORAGE RINGS

The self-consistent overfocusing condition from magnetic fields in a nearly charge-neutralized self-colliding storage ring configuration (Exyder) is now estimated. For simplicity we consider a system where particles are stored within a region $r\lesssim r_0$, the magnetic field is negligibly small, and the particles are turned around by a uniform vacuum magnetic field B_0 that is taken as constant for $r>r_0$. The turning radius in this magnetic field is $r_L=v/\omega_c$ with $\omega_c=qB_0/|\gamma mc$. We assume $r_L\ll r_0$, and the focusing force due to the vacuum magnetic fields is ignored. It can be shown that such a focusing force causes a more restrictive overfocusing condition than we calculate. It is possible that a self-colliding system would not be totally neutralized. The space charge density is then gqn, where g is the fraction of non-neutralization. If this non-neutral component can be controlled, we can compensate the magnetic overfocusing forces with defocusing electric forces, as will be illustrated.

The magnetic flux function for the configuration described is

$$\psi=\begin{cases}0, & r<r_0\\ \frac{1}{2}B_0(r^2-r_0^2), & r>r_0\end{cases}. \tag{29}$$

The particle and current densities are taken to be constant in z between $-\Delta z/2<z<\Delta z/2$, and zero otherwise. The radial structure is given by

$$n=\frac{\bar{n}vr_0}{2r[v^2-(q\psi(r)/(\gamma mrc))^2]^{1/2}}, \tag{30}$$

$$j_\theta=\frac{\bar{n}vr_0q^2\psi(r)}{2\gamma mcr^2[v^2-(q\psi(r)/(\gamma mrc))^2]^{1/2}}, \tag{31}$$

where $\bar{n}$ is the average ion density in the disc, i.e. $\bar{n}\doteq N_T/(\pi r_0^2\,\Delta z)$, N_T is the total number of particles stored. We have used the density and current of an ideally focused system. Using distribution functions the formulas can be modified (as in the previous section) to take into account peaked but finite spreads in phase space.

Substituting for ψ, we have

$$j_\theta = \begin{cases} 0, & r < r_0 \\ -\dfrac{q\bar{n}r_0 v\omega_c(r^2 - r_0^2)}{4r^2[v^2 - \omega_c^2(r^2 - 2r_0^2 + r_0^4/r^2)/4]^{1/2}}, & r_0 + r_L > r > r_0 \end{cases}. \tag{32}$$

Using $\partial B_r/(\partial z) \doteqdot 4\pi j_\theta/c$ and $\partial E_z/\partial z = 4\pi ngqz$, we find for $-\Delta z/2 < z < \Delta z/2$,

$$B_r = \begin{cases} 0, & r < r_0 \\ -\dfrac{2\pi q\omega_c}{rc} n(r)(r^2 - r_0^2)z, & r_0 + r_L > r > r_0 \end{cases}, \tag{33}$$

$$E_z \equiv 4\pi n(r)g(r)zq.$$

The axial force per unit relativistic mass on a particle is

$$\frac{F_z}{\gamma m} = \frac{-q(v_\theta B_r/c - E_z)}{\gamma m}$$

$$= \begin{cases} \dfrac{4\pi n(r)q^2 g(r)z}{m\gamma}, & r < r_0 \\ -\dfrac{\pi q^2\omega_c^2}{\gamma mc^2 r^2} n(r)(r^2 - r_0^2)^2 z + \dfrac{4\pi n(r)q^2 g(r)z}{m\gamma}, & r_0 + e_L > r > r_0 \end{cases}. \tag{34}$$

If $g(r = 0) = 0$, we can use the impulse method developed in Section 2 for determining the overfocusing condition, because then the most significant axial forces occur near the outer particle turning point. If $g(r = 0) \neq 0$, the use of the impulse method is more complicated as particles can move an appreciable distance in z between impulses at $r \approx r_0 + r_L$ and near $r \approx b$. For simplicity we will study only the case where the impulse is only at the outer periphery.

The axial impulse, Δv, is

$$\Delta v = \int_{-T/2}^{T/2} \frac{F_z\, dt}{\gamma m}$$

$$= -\frac{2\pi q^2 z}{\gamma m} \int_0^{r_0 + r_L(1-\varepsilon)} \frac{dr[\omega_c^2 n(r)(r^2 - r_0^2)^2\theta(r - r_0)/r^2c^2 - 4g(r)n(r)]}{r^2[v^2 - \omega_c^2\theta(r - r_0)(r^2 - r_0^2)^2/4r^2]^{1/2}}$$

$$= -\frac{\pi q^2\bar{n}vr_0 z}{\gamma m} \int_0^{r_0 + r_L(1-\varepsilon)} \frac{dr[(r^2 - r_0^2)^2\theta(r - r_0)\omega_c^2/c^2 - 4g(r)r^2]}{r^3[v^2 - \omega_c^2\theta(r - r_0)(r^2 - r_0^2)^2/4r^2]}, \tag{35}$$

where $\theta(x)$ is a step function. These integrals have logarithmically divergent parts near $r = r_0 + r_L$ and near $r = 0$. For $r \approx r_0$ we use $r = r_0 + x$ and $r^2 - r_0^2 \doteqdot 2r_0 x$. Assuming $x \ll r_0$, we find

$$\Delta v = -\frac{4\pi q^2\bar{n}vz}{\gamma m}\left[\int_0^{r_L(1-\varepsilon)} \frac{dx}{(v^2 - \omega_c^2 x^2)}\left(\frac{\omega_c^2 x^2}{c^2} - g_1\right)\right]$$

$$\doteqdot -\frac{2\pi q^2\bar{n}vr_L z}{\gamma mc^2}\ln\left(\frac{1}{\varepsilon}\right)\left[1 - \frac{c^2 g_1}{v^2}\right] = -\frac{\alpha\beta}{4}\omega_c z\ln\left(\frac{1}{\varepsilon}\right), \tag{36}$$

where $\alpha = 1 - g_1 c^2/v^2$, $\varepsilon = \Delta z/r_L + b/r_0$, $g_1 = g(r_0 \div r_0 + e_L)$, b is the spread of the impact parameter, and $\bar{\beta} = 8\pi\bar{n}m\gamma v^2/B_0^2$. The cut-off parameter is determined as follows. At $r \approx r_0 + r_L \equiv r_1$ there is an axial width Δz. Our expression for B_r and E_z requires $\Delta z \partial n/\partial r < n$, which restricts $r_1 - r > \Delta z$. In addition, if there is a spread in the impact parameter b, the turning points near $r = r_0 + r_L$ are smeared by a distance $\approx br_L/r_0$. Thus the expression for the impulse near the outer periphery breaks down a distance $\varepsilon r_L \approx \Delta z + br_L/r_0$ from r_1. The period of a radial bounce is $T = 2r_0/v$; Therefore stability against overfocusing, $|\Delta v/z|\, T < 4$, requires

$$\bar{\beta} < \frac{r_L}{r_0} \frac{8}{\ln(1/\varepsilon)\alpha}. \tag{37}$$

Eq. (37) implies a limit on the luminosity of the Exyder storage ring. The luminosity is defined as

$$\begin{aligned} L &= c\int d^3 r n^2 \\ &\div \frac{2\pi c}{4} \bar{n}^2 r_0^2 \Delta z \int_{\varepsilon_1 r_0}^{r_0} \frac{dr}{r} \\ &= \frac{2\pi c}{4} \bar{n}^2 r_0^2 \Delta z \ln\left(\frac{1}{\varepsilon_1}\right) \div \frac{2\pi}{4} \frac{\bar{\beta}^2 B_0^4 r_0^2 \Delta z \ln(1/\varepsilon_1)}{(8\pi)^2 m^2 \gamma^2 c^3}, \end{aligned} \tag{38}$$

where $\varepsilon_1 = b/r_0$ and we assume $\gamma \gg 1$. Thus, using Eq. (37), the luminosity is limited to

$$L < \frac{B_0^4 r_L^2 \Delta z \ln(1/\varepsilon_1)}{2\pi \ln^2(1/\varepsilon) m^2 \gamma^2 c^3 \alpha^2} = \frac{\varepsilon_2 \ln(1/\varepsilon_1)}{\ln^2(1/\varepsilon)} \frac{\gamma B_0^4}{2\pi \omega_{cr}^3 m^2 \alpha^2}, \tag{39}$$

where $\varepsilon_2 = \Delta z/r_L$ and $\omega_{cr} = (qB/mc)$. As an example, consider $B_0 = 5 \times 10^4$ gauss, $\gamma = 10$, and m is the mass of a proton. We find

$$L < \frac{3.1}{\alpha^2} \times 10^{40} \frac{\varepsilon_2 \ln(1/\varepsilon_1)}{\ln^2(1/\varepsilon)} \frac{\text{cm}^{-2}}{\text{sec}}. \tag{40}$$

Note that for a charge-neutral self-collider, the overfocusing condition limits the luminosity from scaling with radial size. However, a significant increase in luminosity can be achieved if α can be made less than unity. Care with charge neutralization is needed, however, since $\alpha < 0$ causes defocusing.

REFERENCES

1. B. C. Maglich et al., *Phys. Rev. Lett.* **27,** 909 (1971).
2. S. R. Chanon, J. E. Golden, and R. A. Miller, *Phys. Rev. A* **17,** 407 (1978).
3. J. P. Blewett, *Nucl. Instrum. Meth. A* **271,** 212 (1988).
4. B. C. Maglich, *Nucl. Instrum. Meth. A* **271,** 167 (1988).
5. J. P. Blewett, *Part. Accel.* **34,** 13 (1990)
6. H. V. Wong, M. N. Rosenbluth, and H. L. Berk, Stability Thresholds of a Disk-Shaped Migma, *Phys. Fluids B,* **1,** 4 April 1989.